A Complex Low-IF Transceiver Architecture for Relaxing Phase Noise and Settling Time Requirements of RF PLL-FS

Pui-In Mak, Ka-Hou Ao Ieong, Chong-Yin Fok, Seng-Pan U [1] and R. P. Martins [2]

Analog and Mixed-Signal VLSI laboratory, FST, University of Macau, Macau SAR, China (E-mail –p.i.mak@ieee.org)
1 – Also with Chipidea Microelectronics (Macao) Ltd., 2 – On leave from Instituto Superior Técnico, Lisbon, Portugal

Abstract- This paper presents a two-step up/down conversion complex low-IF transceiver architecture. The IF up/down conversion is performed by an I/Q-mismatch-insensitive programmable analog-double quadrature sampling (A-DQS) technique, which shifts the frequency spectrum in the complex domain to reduce the step-size of the PLL frequency synthesizer (PLL-FS) and locking position of the local oscillator (LO), so as to relax the setting time and phase noise requirements. An in-depth mathematical treatment of such a technique will be presented to fully describe the operation and its non-idealities induced image problem.

Keywords- Analog Front-End, Channel Selection, I/Q-mismatch

1. INTRODUCTION

Unrelenting demand for concurrent improvements in wireless transceiver integratability, power consumption, and multistandard compatibility compels engineers to confine the design space with much greater enhancement than in the past. Traditional transceiver architectures, such as super-heterodyne [1], are no longer adequate to satisfy those requirements, thus the research forces trends to the development of monolithic architectures e.g., zero- and low-IF [2]-[5]. In this paper, a monolithic complex wireless low-IF transceiver by using A-DQS technique [6], [7] is proposed, as shown in Fig. 1. Setting the intermediate frequency (IF) equal to half of the channel bandwidth, the desired signal or its image can be selected flexibly from IF to the baseband in the receiver (or in the transmitter from baseband to IF) through simple digital control. The benefits of this channel selection partitioning are 1) the step-size of the PLL-FS can be doubled to two channels bandwidth in order to maintain low phase noise and fast settling time in very low-IF operation, 2) the locking position of the local oscillator in the entire frequency band is halved so as to simplify the frequency divider.

The next section will describe the two-step channel selection mathematically in both transmit and receive modes. The non-ideal A-DQS model will be followed. Then, the circuit implementation and simulation results will be presented. Conclusion will be drawn finally.

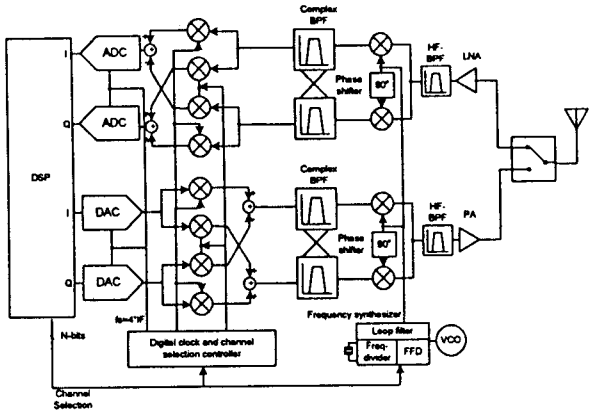

Fig. 1 Two-step channel-select wireless transceiver architecture.

2. CHANNEL SELECTION BY A-DQS

In order to fully illustrate how the frequency shifting property of A-DQS can perform the function of channel selection between two adjacent channels, the mathematical model of A-DQS will be presented in this section.

A. Transmitter up-conversion

The frequency up-conversion and two-step channel selection of proposed transmitter architecture is illustrated in Fig. 2. The baseband input signal, as shown in Fig. 2a, is given by:

$$x(t)\big|_{t=nT} = x_I(t) + j \cdot x_Q(t) \quad n = 0,1,2,... \qquad (1)$$

Next, the signal will face the complex A-DQS that will result in the forward shifting (FS) or backward shifting (BS), the orthogonal samplers $p_I(t)$ and $p_Q(t)$ is expressed as:

$$p_I(t) = \sum_{n=-\infty}^{\infty}[\delta(t-nT_s) - \delta(t-nT_s - T/2)]$$
$$p_Q(t) = \sum_{n=-\infty}^{\infty}[\pm\delta(t-nT_s - T/4) \mp \delta(t-nT_s + T/4)] \qquad (2a\text{-}b)$$

with sampling frequency, $f_s = 4f_{IF}$ as shown in Fig. 3. For FS, it will be necessary to consider the Eq. 2b with the upper sign, whereas for BS, the lower sign must be considered in the same equation and the same rule applies in the following.

On the other hand, in the frequency domain, the Fourier transforms of $p_I(t)$ and $p_Q(t)$ are:

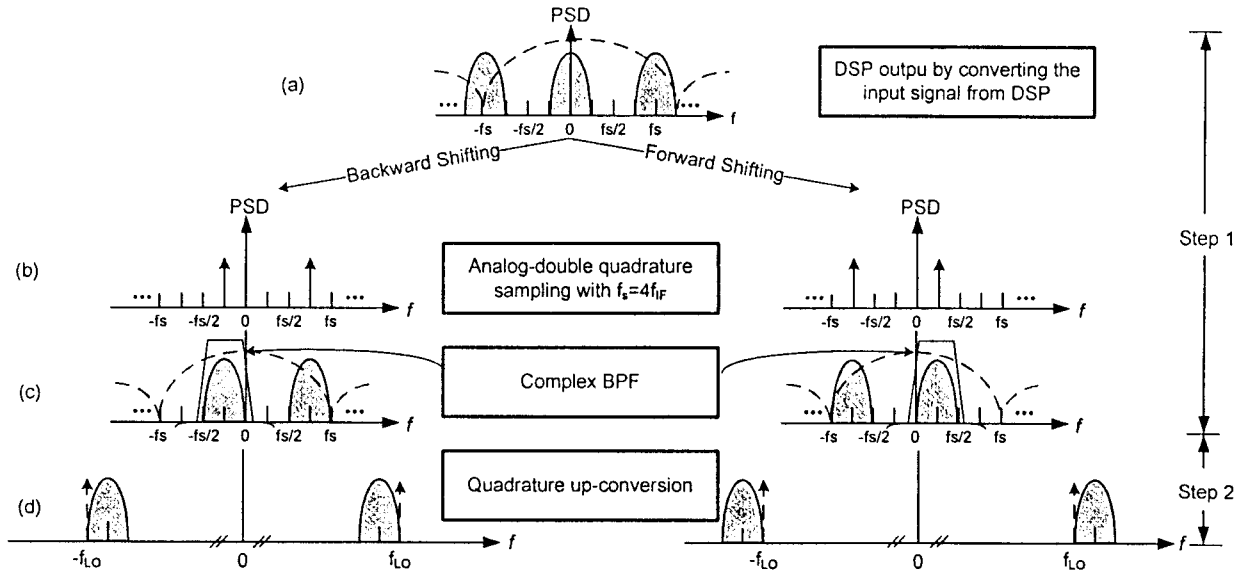

Fig. 2 Proposed frequency up-conversion method and channel selection by A-DQS in transmitter.

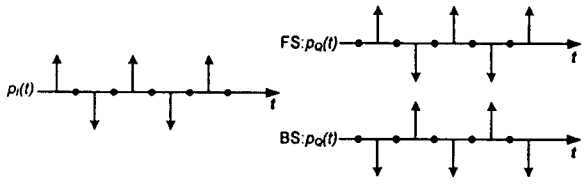

Fig. 3 Complex sampler in the time domain: $p_I(t)$, FS: $p_Q(t)$ for forward shifting and BS:$p_Q(t)$ for backward shifting.

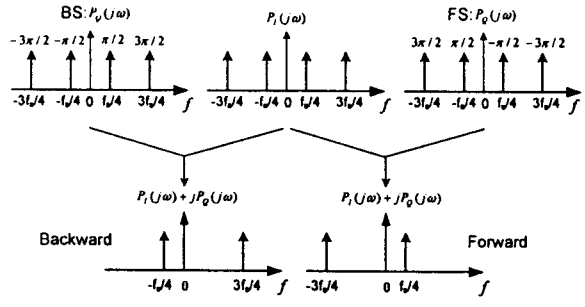

Fig. 4 Frequency domain of samplers $P_I(j\omega)$, *FS:* $P_Q(j\omega)$, *BS:*$P_Q(j\omega)$ and $P_I(j\omega)$+j$P_Q(j\omega)$ for FS and BS.

$$P_I(j\omega) = \sum_{k=-\infty}^{\infty} 2\pi a_k \delta(\omega - k\omega_{IF})$$
$$P_Q(j\omega) = \sum_{k=-\infty}^{\infty} 2\pi b_k \delta(\omega - k\omega_{IF}) \quad (3a\text{-}b)$$

which they are shown in Fig. 4 for FS and BS conditions, where a_k and b_k are the Fourier coefficients,

$$a_k = \begin{cases} \frac{2}{T} & \text{for } k = 2n+1, n = 0,\pm1,\pm2,\cdots \\ 0 & \text{otherwise} \end{cases}$$
$$b_k = \begin{cases} \frac{2}{T} e^{\mp jk\pi k\pi} & \text{for } k = 2n+1, n = 0,\pm1,\pm2,\cdots \\ 0 & \text{otherwise} \end{cases} \quad (4a\text{-}b)$$

The complex sampler $P(j\omega)$ is obtained by combining $P_I(j\omega)$ and $P_Q(j\omega)$, as shown in Fig. 4 also, and it is given by:

$$P(j\omega) = P_I(j\omega) + jP_Q(j\omega) = \sum_{k=-\infty}^{\infty} 2\pi c_k \delta(\omega - k\omega_{IF}) \quad (5)$$

where c_k is the Fourier coefficient,

$$c_k = a_k + jb_k = \begin{cases} 4/T & \text{for } k = 4n\pm1, n = 0,\pm1,\pm2,\ldots \\ 0 & \text{otherwise.} \end{cases} \quad (6)$$

Thus, the complex sampling operation is equivalent to a multiplication of the output by the complex term,

$$cos(n\pi/2) \pm j\, sin(n\pi/2) \quad n = 0,1,2,\ldots \quad (7)$$

The up-converted output then will filtered by the complex bandpass filter (BPF). This filter is not only smoothing the D/A converter (DAC) output, but also compressed I/Q mismatch. The filtered IF output is expressed as:

$$x_{IF}(t) = x_{IF,I}(t) + j \cdot x_{IF,Q}(t) \quad (8)$$

where

$$x_{IF,I}(t) = x_I(t)cos(\omega_{IF}t) \mp x_q(t)sin(\omega_{IF}t)$$
$$x_{IF,Q}(t) = \pm x_I(t)sin(\omega_{IF}t) + x_q(t)cos(\omega_{IF}t) \quad (9a\text{-}b)$$

Then the IF signal is up-converted to RF again by the quadrature complex-to-real up-conversion as:

$$x_{RF}(t) = x_{IF,I}(t) \cdot cos(\omega_{LO}t) + j \cdot x_{IF,Q}(t) \cdot sin(\omega_{LO}t) \quad (10)$$

where ω_{LO} is the PLL local oscillation frequency. The next stage high frequency bandpass filter (HF-BPF) does not necessary required depend on the quality of transmittal. Finally, the signal will flow though the power amplifier (PA) and antenna to transport to RF channel as shown in Fig. 2d.

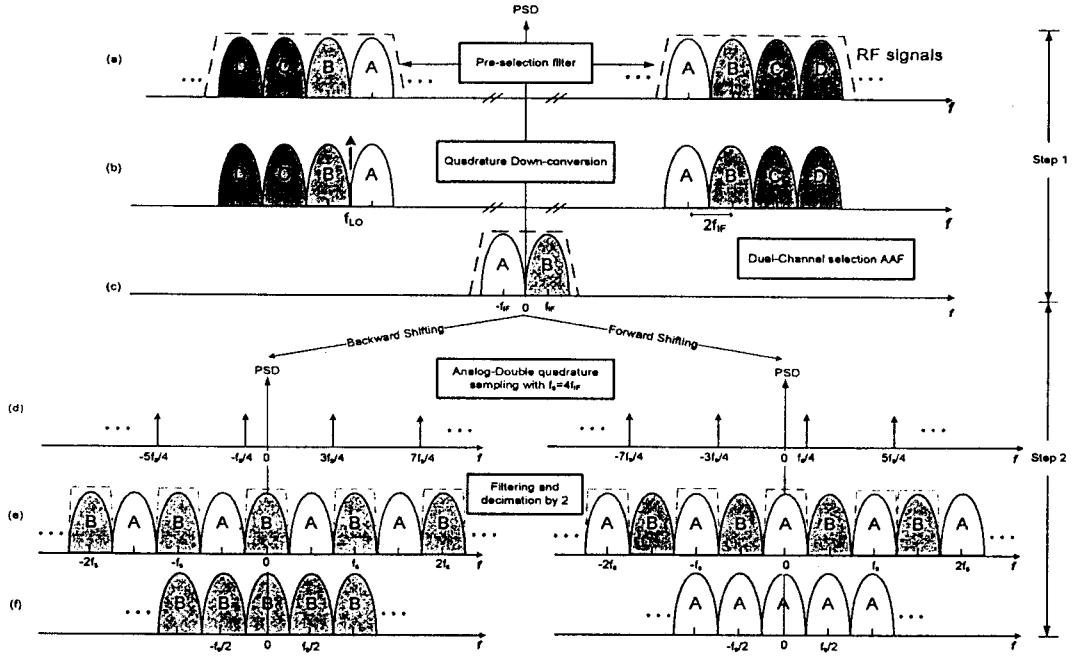

Fig. 5 Proposed frequency down-conversion method and channel selection by A-DQS in receiver.

B. Receiver down-conversion

The down-conversion is just the inverting process of the transmitter, the front-to-back end frequency down-conversion and channel selection are described in Fig. 5. The band-limited RF channels (labeled **A**, **B**, **C** and **D**) in Fig. 5a are first filtered and then amplified by a pre-selection filter and a LNA, respectively. It can be considered also that the desired channels are **A** and **B**, given by:

$$x_{RF}(t) = A(t)\cos[\omega_{SIG}t + \phi_A(t)] + B(t)\cos[\omega_{IMG}t + \phi_B(t)] \quad (11)$$

For coherent detection receivers, Eq. (11) is conveniently re-expressed with two components, in-phase (I) and quadrature-phase (Q) given by:

$$x_{RF}(t) = I_A(t)\cos(\omega_{SIG}t) - Q_A(t)\sin(\omega_{SIG}t) + I_B(t)\cos(\omega_{IMG}t) - Q_B(t)\sin(\omega_{IMG}t) \quad (12)$$

where

$$I_A(t) = A(t)\cos\phi_A(t), Q_A(t) = A(t)\sin\phi_A(t)$$
$$I_B(t) = B(t)\cos\phi_B(t), Q_B(t) = B(t)\sin\phi_B(t) \quad (13a\text{-}d)$$

The dual channel **A** and **B** are then mixed down to the IF by a quadrature down-converter driven LO. The frequency location of the LO is selected between every two channels, such as channel **A** and **B** (Fig. 5b). Thus, channel **B** will be the corresponding image of **A** or vice versa. The key benefit of this IF operation is the low image rejection requirement as the maximum power of the adjacent channel is much smaller than the other in-band channels in most wireless communications.

The down-converted channels **A** and **B** after lowpass filtering by an anti-aliasing filter (AAF), are settled at $-f_{IF}$ and $+f_{IF}$, respectively, as given by:

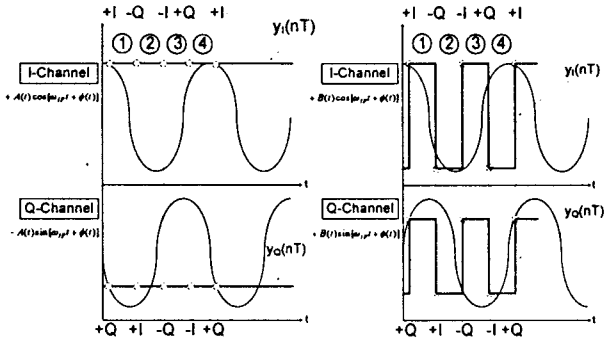

Fig. 6 Forward shifting (a) channel A (b) channel B.

$$x_{IF}(t) = x_{IF,I}(t) + j\cdot x_{IF,Q}(t) = \frac{I_A(t)}{2}e^{-j(\omega_{LO}t+\phi_{LO})} + j\frac{Q_A(t)}{2}e^{-j(\omega_{LO}t+\phi_{LO})} + \frac{I_B(t)}{2}e^{j(\omega_{LO}t+\phi_{LO})} + j\frac{Q_B(t)}{2}e^{j(\omega_{LO}t+\phi_{LO})} \quad (14)$$

Next, the signals will face a complex sampling operation (starting the A-DQS) that will result in a forward and backward shifting, as shown in Fig. 2d, with orthogonal samplers $p_I(t)$ and $p_Q(t)$ in Eq. (2) Leading to the sampled output (Fig. 5f) represented by:

$$x(nT) = [x_{IF,I}(nT)\cos(n\pi/2) \mp x_{IF,Q}(nT)\sin(n\pi/2)] + j[x_{IF,Q}(nT)\cos(n\pi/2) \pm x_{IF,I}(nT)\sin(n\pi/2)] \quad (15)$$

Eq. (11) can be easily demonstrated in the time domain as shown in Fig. 6. Suppose, in forward shifting, two single-harmonic input signals

$$x_{IF}(t) = A(t)e^{-j[\omega_{IF}t+\phi_A(t)]} + B(t)e^{j[\omega_{IF}t+\phi_B(t)]} \quad (16a)$$

$$x_{IF,I}(t) = Re\{x(t)\} = A(t)\cos[\omega_{IF}t + \phi_A(t)] + B(t)\cos[\omega_{IF}t + \phi_B(t)] \quad (16b)$$

$$x_{IF,Q}(t) = Im\{x(t)\} = -A(t)\sin[\omega_{IF}t + \phi_A(t)] + B(t)\sin[\omega_{IF}t + \phi_B(t)] \quad (16c)$$

that are sampled-and-held by the A-DQS. Such *IF* inputs $+IF_i$, $-IF_q$, $-IF_i$, $+IF_q$ are sampled by *I* channel during clock phases, 1,2,3 and 4 respectively; $+IF_q$, $+IF_i$, $-IF_q$, $-IF_i$ are sampled by *Q* channel during clock phases, 1,2,3 and 4 respectively. On the other hand, in the frequency domain, the channel **A** is obtained at $\pm nf_s$ for $n=0,1,2...$whereas channel **B** (image of **A**) is shifted to $\pm nf_s/2$ for $n=1,3,5...$

Similar results can be obtained for backward shifting. Clearly, both cases do not suffer from the DC offset and *1/f* noise problems since those noises are shifted to $\pm nf_s/4$, for $n=1,3,5....$ Finally, after complex sampling through A-DQS followed by A/D conversion, the *I* and *Q* data at a rate $f_s/2$ can be obtained through digital decimation by a factor of two, as shown in Fig. 5e and 5f.

3. REALIZATION OF A-DQS

As mention in the previous section, the A-DQS up/down conversion is easily implemented by the switches, and the channel selection can be effectively realized by exchanging the sampling sequence between clock phase 2 and 4, as shown in Fig. 7. Thus, a simple digital circuit (channel selection controller) controlled by the DSP can be employed to perform such a function.

4. SIMULATION RESULTS

As illustrated above, the channel selection can be effectively realized by exchanging the sampling.

In the transmitter side, two 10 bits oversampling D/A converters were modeled at the system level in a MatlabTM environment and simulated with *Simulink*^{TM}. The input complex signal with $+f_{sig}$ frequency is inserted to the system. The images will repeat occur at the sampling frequency position (f_s) and compressed with the *Sinc* function filter due to the D/A converter is equivalent to operate sample-and-hold function as Fig 8a. Using the inherent shifting property, the signal will up-convert to the f_s+f_{IF} by FS, or shift to the $-f_s+f_{IF}$ by BS, where $f_{IF}=f_s/4$.

In the receiver side, the A-DQS scheme and two 8 bits Nyquist rate A/D converters were modeled at the system level in a *Matlab*^{TM} environment and simulated with *Simulink*^{TM}. Three test tones: channel **A** (image of channel **B**), channel **B** (image of channel **A**) and a zero frequency tone are applied in the simulation as shown in Fig. 7a. The zero-frequency component is applied to test the low frequency noise sensitivity. To acquire the channel **A** in baseband, forward shifting is used and the power spectrum is shown in Fig. 7b. Channel **A** is shifted to $\pm nf_s$ for $n=0,1,2,$ ...while the zero-frequency tone and channel B are shifted to $\pm nf_s/4$ and $\pm nf_s/2$ for $n=1,3,5...$, respectively. A similar result is shown in Fig. 7c for backward shifting. All the results are consistent with the theoretical analysis presented in the previous section.

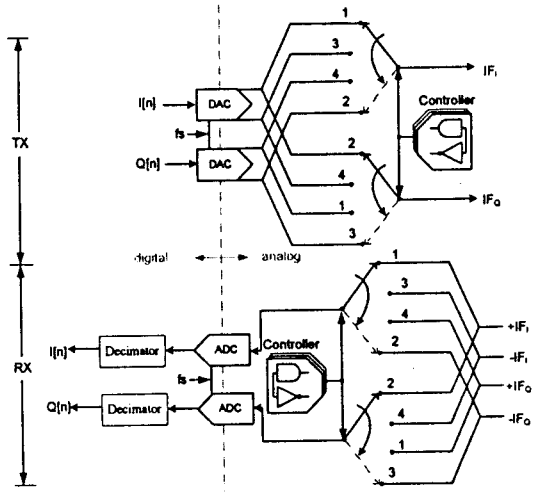

Fig. 7 A-DQS channel selection topology.

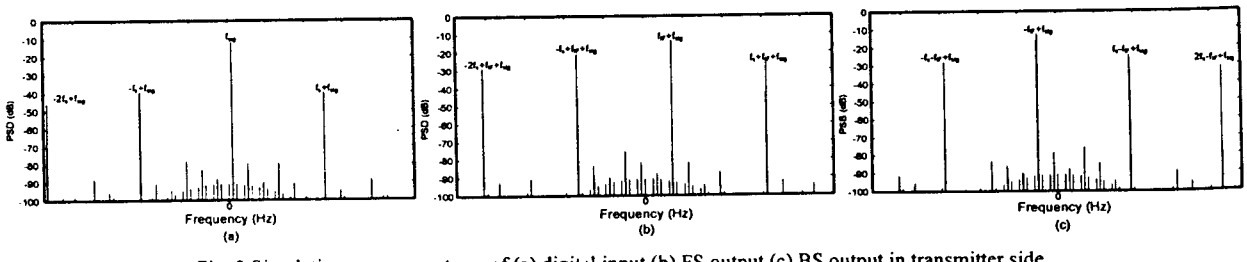

Fig. 8 Simulation power spectrum of (a) digital input (b) FS output (c) BS output in transmitter side.

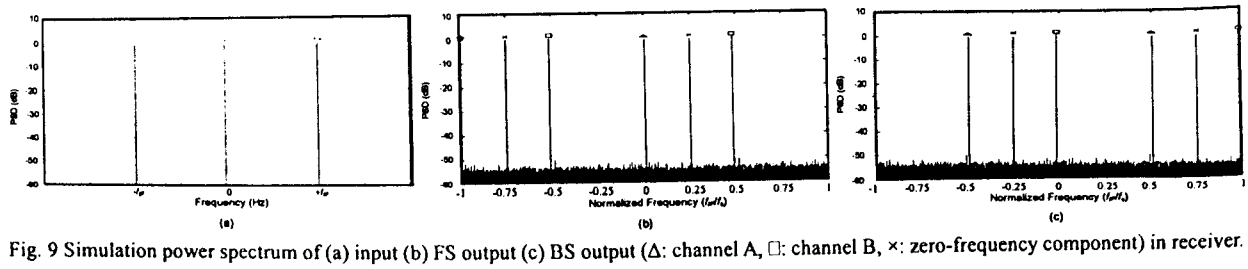

Fig. 9 Simulation power spectrum of (a) input (b) FS output (c) BS output (Δ: channel A, □: channel B, ×: zero-frequency component) in receiver.

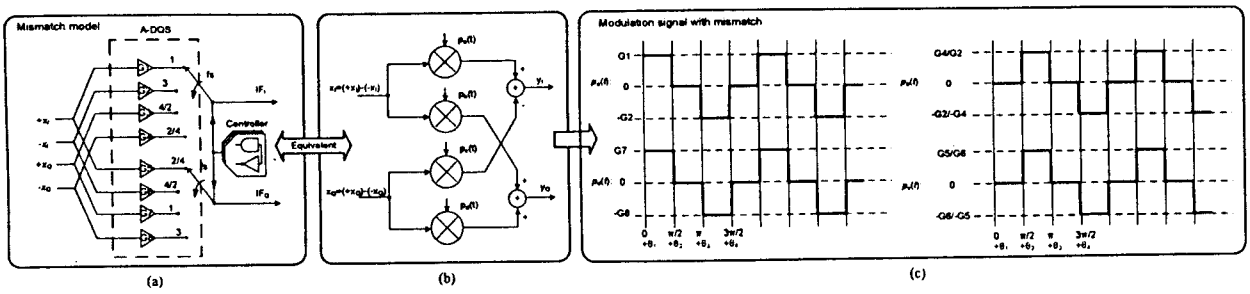

Fig. 10 The equivalent model of A-DQS circuit with mismatch.

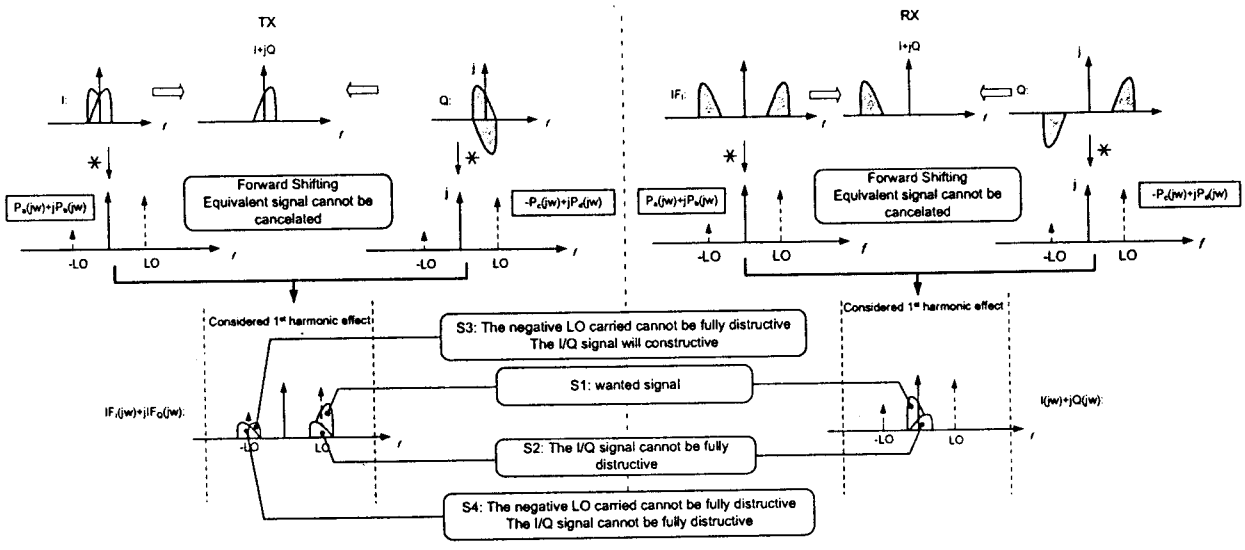

Fig. 11 The A-DQS mismatch analysis in the transmitter and receiver.

5. A-DQS MISMATCH

The cross talk problem in the wireless transceivers employ complex signal (I/Q) for frequency up/down-conversion is unavoidable. The level of I/Q mismatch determines the image-rejection capabilities and its figure of merit is the image-rejection ratio (IRR) given by:

$$\mathrm{IRR} = \frac{P_{\mathrm{Signal}}}{P_{\mathrm{Image(s)}}} \tag{17}$$

A. Gain mismatch

The gain mismatch, which is denote as G1~G8 in Fig. 10, will produce the image cancellation does not be completely in up/down-conversion. That will be decreased IRR performance. Denote the input signal of the A-DQS up/down converter is $x(=x_I+j\cdot x_Q)$ and output signal is $y\ (=y_I+j\cdot y_Q)$. The relation of input and output can be deduced as:

$$\begin{aligned} & y_I + j\cdot y_Q \\ &= \left[x_I\cdot p_a(t) - x_Q\cdot p_c(t)\right] + j\cdot\left[x_I\cdot p_b(t) + x_Q\cdot p_d(t)\right] \\ &= x_I\cdot\left[p_a(t) + j\cdot p_b(t)\right] + x_Q\cdot\left[-p_c(t) + j\cdot p_d(t)\right] \end{aligned} \tag{18}$$

The gain mismatch is assumed static, i.e., it will not varying in time. Thereby, the modulated signal ($p_a(t)$, $p_b(t)$, $p_c(t)$ and $p_d(t)$) are periodic and Fourier series can be applied. The Fourier coefficient of $p_a(t)$ can be deduced as:

$$\begin{aligned} a_k &= \frac{1}{T}\int_T p_a(t)\cdot e^{-jk\omega_0 t}\,dt \\ &= \frac{1}{T}\left[\int_0^{T/4} G_1\cdot e^{-jk\omega_0 t}\,dt - \int_{T/2}^{3T/2} G_2\cdot e^{-jk\omega_0 t}\,dt\right] \\ &= \frac{1}{jk\cdot 2\pi}\left[-G_1\cdot(-j)^k + G_1 + G_2\cdot(j)^k - G_2(-1)^k\right] \end{aligned} \tag{19}$$

The high order harmonic will be compressed by following complex filter in transmitter or digital filter in receiver. The first harmonic is only considered.

$$\begin{aligned} P_a(j\omega)\big|_{1\text{st harmonic}} \approx{}& \frac{G_1+G_2}{\sqrt{2\pi}} e^{-j\frac{\pi}{4}}\cdot\delta\left(j(\omega-\omega_0)\right) + \\ & \frac{G_1+G_2}{\sqrt{2\pi}} e^{j\frac{\pi}{4}}\cdot\delta\left(j(\omega+\omega_0)\right) \end{aligned} \tag{20}$$

Similarly, the first harmonic of the $p_b(t)$ is expressed as:

$$\begin{aligned} P_b(j\omega)\big|_{1\text{st harmonic}} \approx{}& \frac{G_3+G_4}{\sqrt{2\pi}} e^{-j\frac{3\pi}{4}}\cdot\delta\left(j(\omega-\omega_0)\right) + \\ & \frac{G_3+G_4}{\sqrt{2\pi}} e^{j\frac{3\pi}{4}}\cdot\delta\left(j(\omega+\omega_0)\right) \end{aligned} \tag{21}$$

By combining Eq. (20) and Eq. (21), $P_a(j\omega)+jP_b(j\omega)$ is

$$\begin{aligned} & \frac{G_1+G_2+G_3+G_4}{\sqrt{2\pi}} e^{-j\frac{\pi}{4}}\cdot\delta\left(j(\omega-\omega_0)\right) + \\ & \frac{G_1+G_2-G_3-G_4}{\sqrt{2\pi}} e^{-j\frac{\pi}{4}}\cdot\delta\left(j(\omega+\omega_0)\right) \end{aligned} \tag{22}$$

In addition, the other factor of Eq.(18) $-P_c(j\omega)+jP_d(j\omega)$ is

$$\frac{G_5+G_6+G_7+G_8}{\sqrt{2}\pi}e^{j\frac{\pi}{4}}\cdot\delta(j(\omega-\omega_0))+\frac{G_5+G_6-G_7-G_8}{\sqrt{2}\pi}e^{-j\frac{\pi}{4}}\cdot\delta(j(\omega+\omega_0)) \quad (23)$$

The relation between gains and signal magnitude, which includes wanted signal (|S1|) and the image signals (|S2|, |S3| and |S4|) is:

$$|S1|\propto\left|\frac{(G_1+G_2+G_3+G_4)+(G_5+G_6+G_7+G_8)}{\sqrt{2}\pi}\right| \quad (24a)$$

$$|S2|\propto\left|\frac{(G_1+G_2+G_3+G_4)-(G_5+G_6+G_7+G_8)}{\sqrt{2}\pi}\right| \quad (24b)$$

$$|S3|\propto\left|\frac{(G_1+G_2-G_3-G_4)+(G_5+G_6-G_7-G_8)}{\sqrt{2}\pi}\right| \quad (24c)$$

$$|S4|\propto\left|\frac{(G_1+G_2-G_3-G_4)-(G_5+G_6-G_7-G_8)}{\sqrt{2}\pi}\right| \quad (24d)$$

Finally, the effective IRR is the maximum ratio among the wanted signal term to the image ones, i.e. $|S1|^2/|S2|^2$, $|S1|^2/|S3|^2$ and $|S1|^2/|S4|^2$. Moreover, the critical influence is the image power of S2 due to it is directly merged to the signal band and cannot be ameliorated by following stage filter. In the receiver, only $|S1|^2/|S2|^2$ is required to be considered.

B. Phase mismatch

The phase mismatch, as shown in Fig. 10c, will also produce the image to affect the system performance. It makes the converted signal I/Q unbalance shifting, fortunately, the images will not be combined to the signal band. The mathematical expression will be described follows. The assumption is same as gain mismatch analysis; it means the modulated signal is also periodic. The first harmonic components of two important terms in Eq. (18) are;

$$P_a(j\omega)+jP_b(j\omega)=\frac{e^{-j\theta_1}+e^{-j\theta_2}+e^{-j\theta_3}+e^{-j\theta_4}}{\sqrt{2}\pi}e^{-j\frac{\pi}{4}}\cdot\delta(j(\omega-\omega_0))+\frac{-e^{j\theta_1}+e^{j\theta_2}-e^{j\theta_3}+e^{j\theta_4}}{\sqrt{2}\pi}e^{-j\frac{\pi}{4}}\cdot\delta(j(\omega+\omega_0)) \quad (25)$$

and

$$-P_c(j\omega)+jP_d(j\omega)=\frac{e^{-j\theta_1}+e^{-j\theta_2}+e^{-j\theta_3}+e^{-j\theta_4}}{\sqrt{2}\pi}e^{j\frac{\pi}{4}}\cdot\delta(j(\omega-\omega_0))+\frac{-e^{j\theta_1}+e^{j\theta_2}-e^{j\theta_3}+e^{j\theta_4}}{\sqrt{2}\pi}e^{j\frac{\pi}{4}}\cdot\delta(j(\omega+\omega_0)) \quad (26)$$

The signal and image powers can be calculated as:

$$|S1|\propto\left|\frac{e^{-j\theta_1}+e^{-j\theta_2}+e^{-j\theta_3}+e^{-j\theta_4}}{\sqrt{2}\pi}\right| \quad (27a)$$

$$|S2|\propto 0 \quad (27b)$$

$$|S3|\propto\left|\frac{-e^{-j\theta_1}+e^{-j\theta_2}-e^{-j\theta_3}+e^{-j\theta_4}}{\sqrt{2}\pi}\right| \quad (28c)$$

$$|S4|\propto 0 \quad (28d)$$

To deserve to be mentioned, the IRR is only required to consider $|S1|^2/|S3|^2$

6. CONCLUSION

The IF channel selection technique for complex transceiver by utilizing an analog double quadrature sampling technique has been presented. This technique allows the implementation of channel selection through the exchange of the sampling sequence with simple digital controls, such that the step-size of the frequency synthesizer is kept high, maintaining low phase noise and fast settling time, with the required half number of locking positions for the local oscillator. The principle is verified by *Matlab*™ simulations and is applicable to both transmitter/receiver for frequency up/down-conversion at low-IF.

ACKNOWLEDGMENT

This work is financially supported by the *University of Macau* under the research grant with Ref. No. RG069/02-03S/MR/FST.

REFERENCES

[1] T. Okanobu, *et al.* "A Complete Single-Chip AM/FM Radio Integrated Circuit," *IEEE Transactions on Consumer Electronics*, vol. CE-28, pp.393-408, August 1982

[2] J. Ryynänen, *et al.*, "A single-chip multimode receiver for GSM900, DCS1800, PCS1900, and WCDMA," *IEEE Journal of Solid-state Circuits*, vol. 38, no. 4, April 2003.

[3] Won Namgoong and Teresa H. Meng "Direct-Conversion RF receiver Design," *IEEE Transaction on communications*, vol. 49, no.3, March 2001.

[4] Jan Crols and M. Steyaert "Low-IF Topologies for High-Performance Analog Front Ends of Fully Integrated Receivers," *IEEE Transaction on Circuit and Systems-II*, vol.45, no.3, March 1998.

[5] Jan Crols and M. Steyaert "A Single-Chip 900MHz CMOS Receiver Front-End with a High Performance Low-IF topology," *IEEE Journal of Solid-State Circuits*, vol. 30, no. 12, December 1995.

[6] C. A. Leme, Ricardo Reis and Eduardo Viegas "Wide-band sub-sampling A/D conversion with image rejection," *in IEEE Workshop on Wireless Communication Circuits and Systems*, Lucerne, Switzerland, June 1998.

[7] Kong-Pang Pun, *et al.* "A Quadrature Sampling Scheme with Improved Image Rejection for Complex-IF Receivers," *IEEE Int. Sym. on Circuits and Systems Sydney*, Australia, May 2001.